How Do Ice Crystals Grow inside Quasiliquid Layers?

Ken-ichiro Murata,* Ken Nagashima, and Gen Sazaki
Institute of Low Temperature Science, Hokkaido University, N19-W8, Kita-ku, Sapporo 060-0819, Japan

(Received 13 March 2018; published 18 January 2019)

A microscopic understanding of crystal-melt interfaces, inseparably involved in the dynamics of crystallization, is a long-standing challenge in condensed matter physics. Here, using an advanced optical microscopy, we directly visualize growing interfaces between ice basal faces and quasiliquid layers (QLLs) during ice crystal growth. This system serves as a model for studying the molecular incorporation process of the crystal growth from a supercooled melt (the so-called melt growth), often hidden by inevitable latent heat diffusion and/or the extremely high crystal growth rate. We reveal that the growth of basal faces inside QLLs proceeds layer by layer via two-dimensional nucleation of monomolecular islands. We also find that the lateral growth rate of the islands is well described by the Wilson-Frenkel law, taking into account the slowing down of the dynamics of water molecules interfaced with ice. These results clearly indicate that, after averaging surface molecular fluctuations, the layer by layer stacking still survives even at the topmost layer on basal faces, which supports the kink-step-terrace picture even for the melt growth.

DOI: 10.1103/PhysRevLett.122.026102

Ice crystallization from supercooled water is one of the most fundamental first order phase transitions seen in our daily lives. This phenomenon is not only familiar to us, but is also an essential player involved in a diverse set of natural phenomena on Earth [1–5]. Its control is also crucially important for cryopreservation of cells, tissues, and organs, and for living things in the cryosphere, which are seriously harmed by ice crystal formation [6]. From a more general perspective, ice crystallization is mapped into a liquid-to-crystal transition (crystallization from its own supercooled melt, often referred to as melt growth), which has historically attracted considerable attentions in materials science because of the link to producing high quality crystals. Thus, the importance of the fundamental understanding of the water-ice phase transition ranges over broad research fields, including biological, geophysical, and material branches.

In general, crystallization is known to have a strong first order nature [7]. So its ordering process is governed by the kinetics of the interface, especially in the late stage after initial nucleation. It is well accepted that the interfacial structure, including the presence of dislocations, plays key roles in the growth process of crystals: adhesive growth on rough interfaces and layerwise growth on facets [8]. The validity of this view has been tested over many years both theoretically and experimentally for the vapor and the solution growth [9]. For the melt growth, however, its validity is not trivial and firm experimental support is still rare [10,11], although the same arguments are expected to hold. This is mainly because the significantly high crystal growth rate in the melt hampers direct and precise observations of the interface. Moreover, even for a low degree of supercooling, effects of the latent heat transfer often obscure the molecular uptake process at the interfacial growth front. Therefore, microscopic understanding of crystal-melt interfaces based on experiments remains a persistent challenge.

Excluding model systems (e.g., numerical simulations [12–18] and colloidal experiments [19–21]), the sole exception is the helium crystal [22], which has been the focus of attention for a long time as an ideal system for examining the nature of crystal-melt interfaces (more generally, the theory of crystal growth), due to the unique properties of helium crystals: the absence of latent heat and the fast relaxation to the equilibrium state. Even for the helium crystal, however, *in situ* observations at the level of elementary steps have not been achieved so far.

Recently, we have demonstrated the underlying mechanism of the formation of quasiliquid layers (QLLs) [23–26] using an advanced optical microscopy (laser confocal microscopy combined with differential interference contrast microscopy: LCM-DIM [27]), whose resolution in the height direction reaches the order of an angstrom. In this Letter, we focus on the growth kinetics of ice crystals inside QLLs as a model for studying the elementary process of the melt growth. Because of the nonequilibrium nature of QLLs [25,26], ice crystals inside QLLs are expected to grow spontaneously. Here, we succeed in direct visualization of the nucleation and growth of 2D islands of one molecule height even inside QLLs as in the vapor growth of ice [28]. This allows us to discuss physical factors governing the step dynamics and their links to the local ordering of water molecules near the interface. Our *in situ* observations provide a significant clue for elucidating the microscopic nature of ice-water interfaces and its role in crystal growth, which has not been experimentally accessible so far.

First, we follow the growth kinetics of an ice basal face in a QLL, whose thickness is 9 nm [29], at $T = -0.5\,^{\circ}\mathrm{C}$, where QLLs exist as a thin layer state [25,26]. This condition is at supersaturation for vapor-ice interfaces, and thus, vapor growth of ice also proceeds simultaneously. Here, note that the wetting state of QLLs is intrinsically the incomplete (pseudopartial) wetting, exhibiting two different morphologies: a thin wetting (adsorbed) layer dominated by the minimum of the interfacial potential, and a droplet with no wetting layer [26]. In this Letter, *in situ* observations of ice surfaces are made by LCM-DIM in an observation chamber, allowing us to adjust the temperature (T) and water vapor pressure (p) of the sample independently [30]. Figure 1 shows the coalescence of two individual 2D islands randomly nucleated from the existing basal face (see, also, Video S1 [30]). We find that, when the steps of the two islands meet, the contrast of the coalescent part always disappears completely. This behavior is characteristic of typical nucleation and layer by layer growth of 2D islands as is observed in the vapor growth of ice [28]. The observation of 2D homogeneous nucleation of islands clearly indicates that the height of the island corresponds to one molecule, that is, the DIM contrasts in the QLL are the genuine elementary step (see Ref. [28], for a detailed discussion on the proof of one molecule height). Furthermore, the elementary steps born from the island nucleation are shared on both wet and dry (bare) ice surfaces. Note that bare surfaces here mean ice-vapor interfaces [30]. These facts indicate that, even in QLLs, the ice basal face is not rough but retains the layer by layer stacking as is the case for ice (basal)-vapor interfaces [23].

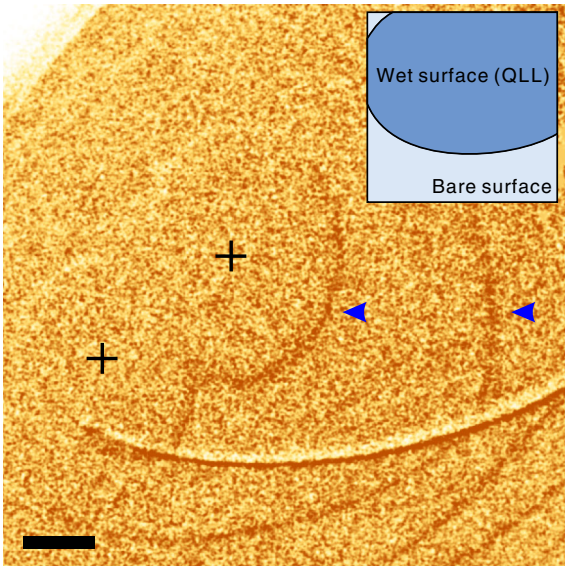

FIG. 1. Homogeneous nucleation and growth of monomolecular islands inside a thin layer type QLL on a basal face at $T = -0.5\,^{\circ}\mathrm{C}$ and $p = 670$ Pa. The cross marks indicate the positions where the 2D islands are nucleated. The blue arrows indicate elementary steps inside the QLL. The inset is a schematic of the image. The scale bar corresponds to 20 μm.

From Video S1 [30], we estimate the nucleation rate of monomolecular islands inside QLLs, J_{QLL}, as $5.24 \times 10^{7}\ \mathrm{m^{-2}\,s^{-1}}$ ($T = -0.5\,^{\circ}\mathrm{C}$ and $p = 670$ Pa). In general, the nucleation rate, J, is linked to the step free energy (the line tension of the step), κ, through the classical 2D nucleation theory, which allows us to determine the step free energy in QLLs (the line tension of the elementary step in QLLs), κ_s', as 3.4×10^{-12} J/m.

In Fig. 2(a), we can see the step perturbation at the boundary due to the difference in the line tension between the elementary step on the bare basal face and the one inside QLLs. In analogy with the Young-Dupré equation for wetting [33], the force balances among these line tensions are expected to hold at the boundary. The force balance in the direction perpendicular to the boundary is written as $\kappa_s \sin\theta = \kappa_s' \sin\theta'$ while that in the parallel direction is expressed as $\kappa_s \cos\theta = \kappa_s' \cos\theta' + \kappa_l$. Here, κ_s and κ_l are the line tensions of the elementary step on the bare basal face and that of the QLL [30], and θ and θ' are the angle of the bare elementary step with respect to the tangent of the boundary and that of the elementary step in QLLs, respectively. In our observations, the values of θ and θ' are estimated as $18^{\circ} \pm 2^{\circ}$ and $58^{\circ} \pm 7^{\circ}$. Inserting $\kappa_s' = 3.4 \times 10^{-12}$ J/m estimated before in the above ratios, we obtain the values of κ_s and κ_l as 9.4×10^{-12} J/m and 7.1×10^{-12} J/m, respectively. These values roughly agree with those independently given by a general relation between the line tension and the interfacial tension, $\kappa = \gamma a$, which yields $\kappa_s' = 12 \times 10^{-12}$ J/m, $\kappa_s = 40 \times 10^{-12}$ J/m and $\kappa_l = 29 \times 10^{-12}$ J/m, respectively [34,37] (a being the lattice constant of the ice basal face, 0.37 nm).

Next, we consider the rate-limiting process responsible for the step dynamics in QLLs from the direct measurement of the step advancing velocity, v_{QLL}. For the melt growth, the step advancing velocity, v_s, and its kinetic coefficient,

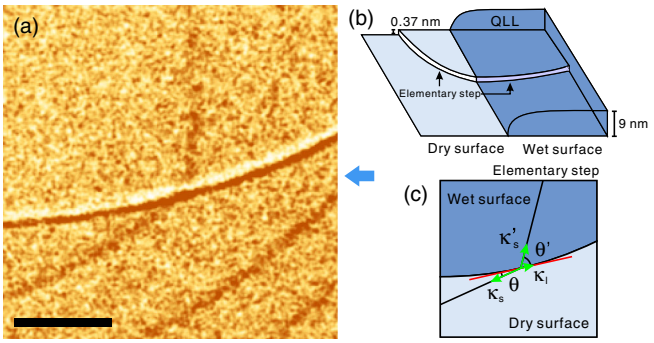

FIG. 2. (a) A perturbation of an elementary step at a boundary between a wet and dry (bare) ice basal face. The scale bar corresponds to 20 μm. (b) A schematic of the image of (a) viewed from the direction of the arrow. (c) A schematic of the force balance among three line tensions, κ_s, κ_s', and κ_l.

β_T, are classically given by the following expressions, the so-called Wilson-Frenkel law [38,39]:

$$v_s = \beta_T (T_m - T), \tag{1}$$

$$\beta_T = \frac{a}{2\pi}\left(\frac{a}{l_0}\right)\tau^{-1}\frac{L}{RT_m T}\exp\left(-\frac{L}{RT_m}\right), \tag{2}$$

where R is the gas constant, T_m is the melting point (273.15 K for ice), l_0 is the mean kink spacing in the step and L is the latent heat of fusion (6.01 kJ/mol for ice). In our system, a/l_0 is, essentially, unity, that is, the kink spacing completely reaches the lattice constant ($l_0 = a$) [40]. Here, τ means a characteristic time required for the incorporation of a molecule in liquid into a crystal lattice. We note that Eqs. (1) and (2) explain the pure incorporation process, not including the effect of the latent heat diffusion. However, as discussed in the Supplemental Material [30], this effect can be ignored in QLLs.

How should τ be interpreted in our system? In general, the molecular incorporation into the crystal lattice requires material transport, which is controlled by the translational diffusion of an individual molecule (not by the structural relaxation) [42]. For water, Kawasaki and Kim have recently demonstrated that the translational diffusion is coupled to the hydrogen bond breakage time [43]. Furthermore, the disordered network of water, incompatible with the crystal symmetry (e.g., five-membered rings of hydrogen bonded molecules [44]), needs to be broken so that a liquid molecule is incorporated into the crystal lattice (see Fig. 3). Thus, τ can be regarded as the hydrogen bond breakage time of water molecules.

We show, in Fig. 4, the temperature dependence of v_{QLL}. Here, note that the narrow temperature range comes from the fact that thin layer type QLLs are not observed below −2.0 °C [25,26]. In the fitting analysis, τ is dealt as a temperature-independent parameter because of the narrow temperature range, although τ ideally has the temperature dependence (for bulk water, the change in τ in this range is only 3%). We see that the data can be basically fitted by the combination of Eqs. (1) and (2). In the inset, we also directly compare the relaxation time of QLLs estimated conversely from data of v_{QLL} with that of bulk water obtained by dielectric spectroscopy [46–49] (strictly speaking, the relaxation time of a single water dipole [30]). We find that QLLs (8.65×10^{-10} s) have an approximately 90 times longer relaxation time than bulk water (9.40×10^{-12} s at $T = 0.2$ °C [47]). This slowing down corresponds to the increase of 200 times in the shear viscosity of QLLs over bulk water, previously estimated from the relaxation mode of QLLs' contact lines [29], although their factors are somewhat different each other [50]. These facts strongly suggest that water molecules localized near basal faces slow down due to the structural ordering induced by the interface, which is analogous to that in liquids interfaced with foreign crystalline solids, recently confirmed in various systems [15,51,52].

Interestingly, the value of v_{QLL} tells us that the ice growth inside QLLs is very much slower than the bulk melt growth. The normal growth rate (normal to the facet) in the bulk melt, R_{bulk}, reaches 10^{-2}–10^{-7} m/s although the value exhibits considerable variation, depending on researchers [2,53–55]. We can estimate the normal growth rate in QLLs from v_{QLL} by the relation of $R_{\mathrm{QLL}} = a(\pi J_{\mathrm{QLL}}/3)^{1/3} v_{\mathrm{QLL}}^{2/3}$. Employing $J_{\mathrm{QLL}} = 5.24 \times 10^7$ m^{-2} s^{-1} obtained before consequently yields $R_{\mathrm{QLL}} = 1.66 \times 10^{-10}$ m/s ($\ll R_{\mathrm{bulk}}$). This implies that, on bulk basal faces, the enhancement of 2D nucleation occurs upon approaching the thermal

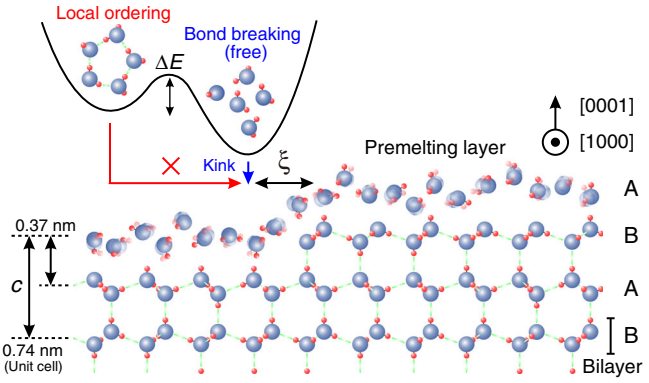

FIG. 3. A schematic illustration explaining the molecular incorporation process into the ice crystal lattice on the basal face. Water molecules in the bond breaking state can be incorporated into kink sites while those in the locally ordered state, frustrated by the ice crystal symmetry, cannot. Thus, overcoming the energy barrier (ΔE) via bond breaking is required for the incorporation. Here, the topmost premelting layer has a finite step width, ξ [45] (see, also, Ref. [30]).

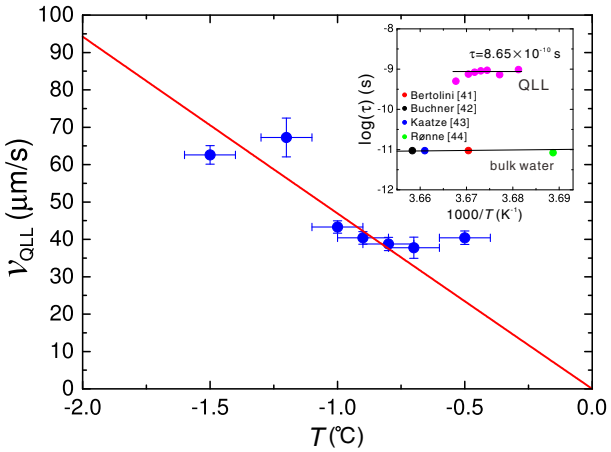

FIG. 4. Temperature dependence of the step advancing velocity in QLLs. The red line indicates the result of the fitting by the combination of Eqs. (1) and (2). The inset shows the comparison of the relaxation time between QLLs and bulk water [46–49] (see, also, Ref. [30]).

roughening transition point [56], although it is located above the melting point for the basal face. The step free energy decreases toward zero when approaching the roughening transition point ($\kappa \to 0$), which reduces the energy barrier for the 2D nucleation, $\Delta G = \pi\Omega\kappa^2/\Delta\mu$, and then results in the drastic increase in the nucleation rate, $J \propto \exp(-\Delta G/k_B T)$ [30]. Recently, Benet *et al.* [57] have demonstrated that long wavelength interfacial fluctuations between ice and QLL are suppressed by the coupling to those between QLL and vapor because of the finite film thickness, which flattens the interface and, thus, suppresses the nucleation rate. This mechanism allows us to make *in situ* observations of the elementary step dynamics even in the melt. We also stress that QLLs cannot exist, even under conditions where their existence is thermodynamically allowable [25,26], if the ice growth rate in QLLs were as fast as the bulk melt growth. This is because the bulk growth rate is supposed to overwhelm the condensation rate from vapor to water (QLL). The moderate growth rate in QLLs avoids this discrepancy and is, therefore, the kinetic origin of the existence of QLLs.

Finally, we remark on the step dynamics inside droplets, appearing in the lower vapor supersaturation regime [25]. Figure 5(a) indicates the transformation of the growth mode from spiral growth to 2D nucleation growth after the appearance of droplets (see, also, Video S2 [30]). Here, we change the temperature and vapor pressure into the range where droplets appear (from $T = -3.1\,^\circ\mathrm{C}$ and $p = 488$ Pa to $T = -2.6\,^\circ\mathrm{C}$ and $p = 509$ Pa), while keeping supersaturated conditions. We find that, after the appearance of droplets, elementary steps running on a bare surface spread concentrically from the droplets, meaning that those can be a source of the 2D nucleation, although the elementary steps in the droplets cannot be visualized due to their round shape. Further supportive evidence for the presence of elementary steps inside droplets is shown in Fig. 5(b) ($T = -1.0\,^\circ\mathrm{C}$ and $p = 567$ Pa). An elementary step initially running on the bare ice surface survives after passing through a droplet while accelerating inside it (see, also, Video S3 [30]). This reveals that elementary steps can exist even under thicker droplets, as is the case for the thin layer type.

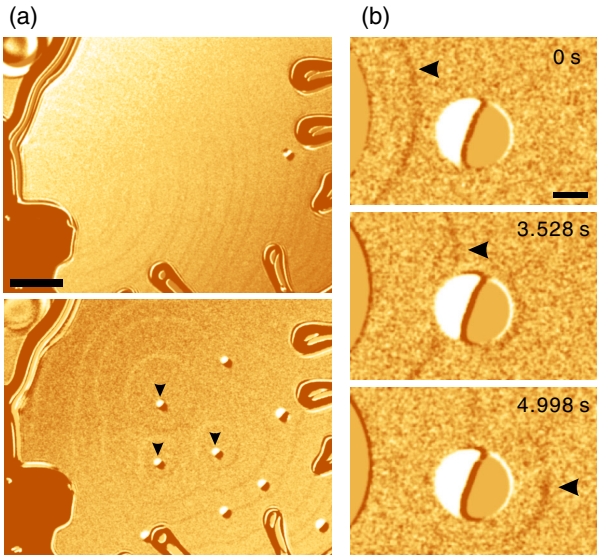

FIG. 5. (a) The transformation of the growth mode on a bare basal face from the spiral growth to the 2D nucleation and growth of the monomolecular islands mediated by droplet type QLLs (see the arrows). The thermodynamic condition for the upper image is $T = -3.1\,^\circ\mathrm{C}$ and $p = 488$ Pa whereas that for the bottom is $T = -2.6\,^\circ\mathrm{C}$ and $p = 509$ Pa. The scale bar corresponds to 20 μm. (b) An elementary step (shown by the arrows) passing through a droplet ($T = -1.0\,^\circ\mathrm{C}$ and $p = 567$ Pa). The step comes from a large droplet next to the central droplet. The scale bar corresponds to 10 μm.

In summary, with the aid of LCM-DIM, we have demonstrated that, inside QLLs, the ice basal face grows layer by layer with accompanying 2D nucleation of monomolecular islands, as is generally observed in vapor and solution growth. This indicates that the averaged positional order of water molecules retains the layer by layer stacking even at the topmost layer, which reveals the relevance of the kink-step-terrace picture even for the melt growth. Moreover, the growth rate of individual elementary steps is dominated by the pure molecular incorporation process obeying the Wilson-Frenkel law, taking into account the increase in the hydrogen bond breakage time of water molecules due to their local ordering near the interface. This slowing down is consistent with the anomalous increase in the shear viscosity of QLLs previously estimated by us [29].

We note that our QLL, the thin wetting layer stabilized by the interfacial potential [26], is distinct from the so-called premelting layer (liquidlike disorder at the topmost layer) at ice-vapor interfaces, which has been intensively studied so far by numerical simulations [58–62] and recently by surface sum-frequency generation (SFG) spectroscopy [63,64]. In our system, the premelting layer is supposed to exist at the topmost layer of bare (and wet) ice surfaces although it is out of the resolution limit of LCM-DIM in the xy direction. In contrast, the numerical simulations and the SFG experiments have not succeeded in detecting the thin wetting layer so far [65]. Our results also pose an interesting question on the microscopic nature of the premelting layer interfacing with liquid water (not water vapor) and its link to the presence of the facet. The difference in the view of the QLL stimulates further broad discussions of the interpretation and the origin of surface melting and the QLL.

The authors are grateful to Y. Saito and K. Ishihara (Olympus Engineering Co., Ltd.) for their technical support of LCM-DIM and G. Layton (Northern Arizona University) for the provision of AgI crystals. This work was partially supported by JSPS KAKENHI Grant Numbers JP16H05979, JP15H02016.

*murata@lowtem.hokudai.ac.jp

[1] U. Nakaya, *Snow Crystals* (Harvard University Press, Cambridge, England, 1954).

[2] H. R. Pruppacher and J. D. Klett, *Microphysics of Clouds and Precipitation* (Kluwer Academic Publishers, Dordrecht, 1997).

[3] *Ice Physics and the Natural Environment*, edited by J. S. Wettlaufer, J. G. Dash, and N. Untersteiner (Springer-Verlag, Berlin, 1999).

[4] H. Morrison, G. de Boer, G. Feingold, J. Harrington, M. D. Shupe, and K. Sulia, Nat. Geosci. **5**, 11 (2012).

[5] T. B. Rausch, V. Bergeron, J. H. E. Cartwright, R. Escribano, J. L. Finney, H. Grothe, P. J. Gutiérrez, J. Haapala, W. F. Kuhs, J. B. C. Pettersson, S. D. Price, C. Ignacio Sainz-Díaz, D. J. Stokes, G. Strazzulla, E. S. Thomson, H. Trinks, and N. Uras-Aytemiz, Rev. Mod. Phys. **84**, 885 (2012).

[6] G. J. Morris and E. Acton, Cryobiology **66**, 85 (2013).

[7] S. Alexander and J. McTague, Phys. Rev. Lett. **41**, 702 (1978).

[8] A. A. Chernov, *Modern Crystallography III* (Springer-Verlag, Berlin, 1984).

[9] A. A. Chernov, J. Cryst. Growth **264**, 499 (2004).

[10] H. Nishizawa, F. Hori, and R. Oshima, J. Cryst. Growth **236**, 51 (2002).

[11] H. Nishizawa, F. Hori, and R. Oshima, Jpn. J. Appl. Phys. **42**, 2805 (2003).

[12] J. J. Hoyt, M. Asta, and A. Karma, Phys. Rev. Lett. **86**, 5530 (2001).

[13] M. Amini and B. B. Laird, Phys. Rev. Lett. **97**, 216102 (2006).

[14] R. Handel, R. L. Davidchack, J. Anwar, and A. Brukhno, Phys. Rev. Lett. **100**, 036104 (2008).

[15] C. Tang and P. Harrowell, Nat. Mater. **12**, 507 (2013).

[16] H. Nada and Y. Furukawa, J. Phys. Chem. B **101**, 6163 (1997).

[17] J. Benet, L. G. MacDowell, and E. Sanz, Phys. Chem. Chem. Phys. **16**, 22159 (2014).

[18] D. T. Limmer and D. Chandler, J. Chem. Phys. **141**, 18C505 (2014).

[19] R. P. A. Dullens, D. G. A. L. Aarts, and W. K. Kegel, Phys. Rev. Lett. **97**, 228301 (2006).

[20] J. H. Guzmán and E. R. Weeks, Proc. Natl. Acad. Sci. U.S.A. **106**, 15198 (2009).

[21] I. B. Ramsteiner, D. A. Weitz, and F. Spaepen, Phys. Rev. E **82**, 041603 (2010).

[22] S. Balibar, H. Alles, and A. Y. Parshin, Rev. Mod. Phys. **77**, 317 (2005).

[23] G. Sazaki, S. Zepeda, S. Nakatsubo, M. Yokomine, and Y. Furukawa, Proc. Natl. Acad. Sci. U.S.A. **109**, 1052 (2012).

[24] G. Sazaki, H. Asakawa, K. Nagashima, S. Nakatsubo, and Y. Furukawa, Cryst. Growth Des. **13**, 1761 (2013).

[25] H. Asakawa, G. Sazaki, K. Nagashima, S. Nakatsubo, and Y. Furukawa, Proc. Natl. Acad. Sci. U.S.A. **113**, 1749 (2016).

[26] K. Murata, H. Asakawa, K. Nagashima, Y. Furukawa, and G. Sazaki, Proc. Natl. Acad. Sci. U.S.A. **113**, E6741 (2016).

[27] G. Sazaki, T. Matsui, K. Tsukamoto, N. Usami, T. Ujihara, K. Fujiwara, and K. Nakajima, J. Cryst. Growth **262**, 536 (2004).

[28] G. Sazaki, S. Zepeda, S. Nakatsubo, E. Yokoyama, and Y. Furukawa, Proc. Natl. Acad. Sci. U.S.A. **107**, 19702 (2010).

[29] K. I. Murata, H. Asakawa, K. Nagashima, Y. Furukawa, and G. Sazaki, Phys. Rev. Lett. **115**, 256103 (2015).

[30] See Supplemental Material at http://link.aps.org/supplemental/10.1103/PhysRevLett.122.026102 for details of our experimental system, characterization, and interpretation of the line tension at the triple line of QLLs, the phenomenological relation between the line tension and the surface tension, latent heat effects inside QLLs, and the structural relaxation time of bulk water, which includes Refs. [31,32].

[31] A. Taschin, P. Bartolini, R. Eramo, and R. Torre, Phys. Rev. E **74**, 031502 (2006).

[32] J. V. Sengers and J. T. R. Watson, J. Phys. Chem. Ref. Data **15**, 1291 (1986).

[33] P. G. de Gennes, F. Brochard-Wyart, and D. Qéré, *Capillarity and Wetting Phenomena: Drops, Bubbles, Pearls, Waves* (Springer-Verlag, New York, 2003).

[34] In this calculation, we employed 109 mN/m [35], 33 mN/m [35], and 76 mN/m [36] as the ice-vapor, the ice-water, and the water-vapor interfacial tensions, respectively, to estimate κ_s, κ_s', and κ_l. In the main text, we employ this relation, not for the quantitative comparison, but for an order of magnitude estimation to confirm the relevance of our values. We further discuss the details of the relation of $\kappa = \gamma a$ in the Supplemental Material.

[35] P. V. Hobbs, *Ice Physics* (Oxford University Press, New York, 1974).

[36] J. Hrubý, V. Vinš, R. Mareš, J. Hykl, and J. Kalová, J. Phys. Chem. Lett. **5**, 425 (2014).

[37] It is worth noting that we can access both κ_s and κ_l, quantities that are extremely difficult to obtain experimentally, once κ_s' is determined.

[38] H. A. Wilson, Philos. Mag. **50**, 238 (1900).

[39] J. Frenkel, Phys. Z. Sowjetunion **1**, 498 (1932).

[40] This is because the elementary steps already undergo the step roughening transition in our temperature regime (see the isotropic shape of the steps in Fig. 1), indicative of step roughening. Note that the roughening transition temperature of the elementary step is at least lower than $T = -26.0\,°\mathrm{C}$ [41].

[41] M. Inomata, K. Murata, H. Asakawa, K. Nagashima, S. Nakatsubo, Y. Furukawa, and G. Sazaki, Cryst. Growth Des. **18**, 786 (2018).

[42] H. Tanaka, Phys. Rev. E **68**, 011505 (2003).

[43] T. Kawasaki and K. Kim, Sci. Adv. **3**, e1700399 (2017).

[44] J. Russo and H. Tanaka, Nat. Commun. **5**, 3556 (2014).

[45] V. Tsepelin, H. Alles, A. Babkin, R. Jochemsen, A. Y. Parshin, and I. A. Todoshchenko, J. Low Temp. Phys. **129**, 489 (2002).

[46] D. Bertolini, M. Cassettari, and G. Salvetti, J. Chem. Phys. **76**, 3285 (1982).

[47] R. Buchner, J. Barthel, and J. Stauber, Chem. Phys. Lett. **306**, 57 (1999).

[48] U. Kaatze, J. Chem. Eng. Data **34**, 371 (1989).

[49] C. Rønne, L. Thrane, P.-O. Åstrand, A. Wallqvist, K. V. Mikkelsen, and S. R. Keiding, J. Chem. Phys. **107**, 5319 (1997).

[50] This mismatch may come from the difference in what dynamics is reflected in these two works. This work measures the relaxation time of the dynamics of water molecules near ice-QLL interfaces, whereas the shear viscosity determined by the wetting dynamics corresponds to that of QLLs themselves, including not only ice-QLL interfaces, but also QLL-vapor interfaces. Because of their hydrophobic nature, QLL (water)-vapor interfaces induce the structural ordering of water molecules near their interfaces, which are expected to contribute to the additional increase in the shear viscosity over the estimation of this work.
[51] W. D. Kaplan and Y. Kauffmann, Annu. Rev. Mater. Res. **36**, 1 (2006).
[52] D. T. Limmer, A. P. Willard, P. Madden, and D. Chandler, Proc. Natl. Acad. Sci. U.S.A. **110**, 4200 (2013).
[53] W. B. Hilling, *Growth and Perfection of Crystals*, edited by R. H. Doremus, B. W. Roberts, and D. Turnbull (Wiley, New York, 1958), pp. 350–360.
[54] E. Yokoyama, I. Yoshizaki, T. Shimaoka, T. Sone, T. Kiyota, and Y. Furukawa, J. Phys. Chem. B **115**, 8739 (2011).
[55] D. Rozmanov and P. G. Kusalik, J. Chem. Phys. **137**, 094702 (2012).
[56] P. E. Wolf, F. Gallet, S. Balibar, E. Rolley, and P. Noziéres, J. Phys. **46**, 1987 (1985).
[57] J. Benet, P. Llombart, E. Sanz, and L. G. MacDowell, Phys. Rev. Lett. **117**, 096101 (2016).
[58] H. Nada and Y. Furukawa, Surf. Sci. **446**, 1 (2000).
[59] T. Ikeda-Fukazawa and K. Kawamura, J. Chem. Phys. **120**, 1395 (2004).
[60] M. M. Conde, C. Vega, and A. Patrykiejew, J. Chem. Phys. **129**, 014702 (2008).
[61] W. Pfalzgraff, S. Neshyba, and M. Roeselova, J. Phys. Chem. A **115**, 6184 (2011).
[62] I. Pickering, M. Paleico, Y. A. P. Sirkin, D. A. Scherlis, and M. H. Factorovich, J. Phys. Chem. B **122**, 4880 (2018).
[63] M. A. Sánchez, T. Kling, T. Ishiyama, M.-J. van Zadel, P. J. Bisson, M. Mezger, M. N. Jochum, J. D. Cyran, W. J. Smit, H. J. Bakker, M. J. Shultz, A. Morita, D. Donadio, Y. Nagata, M. Bonn, and E. H. G. Backus, Proc. Natl. Acad. Sci. U.S.A. **114**, 227 (2017).
[64] W. J. Smit and H. J. Bakker, Angew. Chem. Int. Ed. **129**, 15746 (2017).
[65] For numerical simulations, this comes from the limitation of the computational time and the system size. Note that the time scale of the formation of mesoscopic wetting layers is of the order of milliseconds or seconds, and its spatial scale is of the order of micrometers. This spatiotemporal scale is not accessible with current numerical simulations. For the SFG experiments, thermodynamic conditions are limited to the ice-vapor equilibrium where the presence of mesoscopic wetting layers are not allowable [26] because of the nature of the observation chamber.